Inorganic Chemistry

ARTICLE

pubs.acs.org/IC

Controllable and Reversible Inversion of the Electronic Structure in Nickel *N*-Confused Porphyrin: A Case When MCD Matters

Saovalak Sripothongnak,[†] Christopher J. Ziegler,*[,†] Michael R. Dahlby,[‡] and Victor N. Nemykin*[,‡]

[†]Department of Chemistry, University of Akron, Akron, Ohio 44325-3601, United States

[‡]Department of Chemistry & Biochemistry, University of Minnesota Duluth, Duluth, Minnesota 55812, United States

Supporting Information

ABSTRACT: Nickel *N*-confused tetraphenylporphyrin, **1**, and nickel 2-*N*-methyl-*N*-confused tetraphenylporphyrin, **1-Me**, exhibit unusual sign-reversed (positive-to-negative intensities in ascending energy) MCD spectra in the Q-type band region, suggesting a rare ΔHOMO < ΔLUMO relationship between π and π^* MOs in the porphyrin core. Simple and reversible deprotonation of the external NH proton in **1** dramatically changes the electronic structure of the porphyrin core into the ΔHOMO > ΔLUMO combination characteristic for the *meso*-(tetraaryl)porphyrins. DFT, time-dependent DFT, and semiempirical ZINDO/S calculations on **1**, **1-Me**, and **1**$^-$ confirm the experimental finding and successfully explain the MCD pattern in the target compounds.

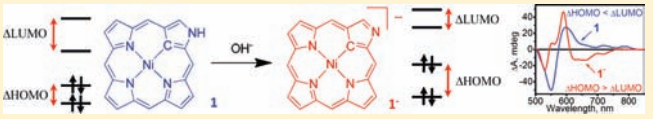

INTRODUCTION

N-Confused porphyrin, also known as inverted porphyrin and 2-aza-21-carbaporphyrin, is one of the most intensively studied isomers of normal porphyrin.[1] In this macrocycle, one of the pyrrole rings is inverted relative to normal porphyrin, such that a β-pyrrolic carbon atom resides at the core of the porphyrinoid and the pyrrolic nitrogen atom occupies a position at the periphery of the macrocycle. In spite of its structural similarity with normal porphyrin, the inversion of a single pyrrole ring clearly alters the electronic structure of the macrocycle, resulting in unique chemical and physical properties.[2] Notwithstanding these striking electronic differences from normal porphyrin, there have been only a limited number of spectroscopic and theoretical studies on the electronic structure of *N*-confused porphyrin free base, and even fewer investigations are available on such properties of its metal complexes.[3]

When coupled with UV−vis spectroscopy, magnetic circular dichroism (MCD) spectroscopy has proven to be useful for understanding of electronic structure of porphyrins and their analogues.[4] The majority of features in the UV−vis and MCD spectra of transition-metal 5,10,15,20-tetra(aryl)porphyrins with effective 4-fold symmetry (i.e., D_{4h}) can be explained using classic Gouterman's four-orbital[5] and Michl's perimeter[6] models. Specifically, in the above case, the porphyrin core-centered LUMO and LUMO+1 π^* MOs are doubly degenerate (ΔLUMO = 0), while the HOMO and HOMO−1 π MOs are nearly degenerate (ΔHOMO ∼ 0). Excited states originating from $a_{1u} \rightarrow e_{gy}$ and $a_{2u} \rightarrow e_{gx}$ transitions have *x*-polarization, while those between $a_{1u} \rightarrow e_{gx}$ and $a_{2u} \rightarrow e_{gy}$ orbitals are *y*-polarized (Figure 1a). The *x*- and *y*-polarized excited states are further mixed and split in energy by configuration interactions into two pairs of degenerate ^1E_u symmetry low-energy, low-intensity Q_x and Q_y transitions, and high-energy, high-intensity B_x and B_y (also known as Soret band) transitions.[5] In the MCD spectra of such compounds, a negative-to-positive intensity pattern (in ascending energy) for Q- and B-bands is predicted by perimeter model,[6] and such a pattern was experimentally observed for numerous transition-metal porphyrins.[7] Lowering the effective symmetry in *N*-confused porphyrins from D_{4h} to C_s (planar *N*-confused porphyrin core) or C_1 (nonplanar *N*-confused porphyrin core) results in nondegeneracy of the porphyrin core-centered LUMO and LUMO+1 MOs and further splitting of Q_x and Q_y as well as B_x and B_y transitions (Figure 1b,c). In order to avoid confusion, when the target low-symmetry porphyrins are discussed below, the generalized notation proposed by Gouterman[5] will be used (i.e., b_1, b_2, c_1, and c_2 for a_{1u}, a_{2u}, e_{gx}, e_{gy} in D_{4h} symmetry; Figure 1). Depending on the nature of substituents attached to the porphyrin core and/or central metal, two possible MCD patterns for *N*-confused porphyrins should be considered.[6] If ΔLUMO < ΔHOMO, a negative-to-positive amplitude of MCD spectrum in ascending energy should be observed for both Q- and B-band regions (Figure 1b), and this is the typical case for the low-symmetry porphyrin compounds.[7] If ΔLUMO > ΔHOMO, a positive-to-negative amplitude MCD spectrum in ascending energy should be observed (Figure 1c), which represents a rare case in porphyrin chemistry. Specifically, such "sign-reversed" MCD spectra were noted in several highly nonplanar porphyrins,[8a,b] expanded and isomeric porphyrins,[8c−e] and reduced porphyrins.[8f] In addition, sign-reversed MCD spectra were recently reported for copper complexes of cis- and trans-doubly *N*-confused porphyrins.[9] To the best of our knowledge, however, there are no reports available in which the electronic structure of the *N*-confused porphyrin core could be reversibly

Received: December 21, 2010
Published: June 24, 2011

dx.doi.org/10.1021/ic102255k | *Inorg. Chem.* 2011, 50, 6902–6909

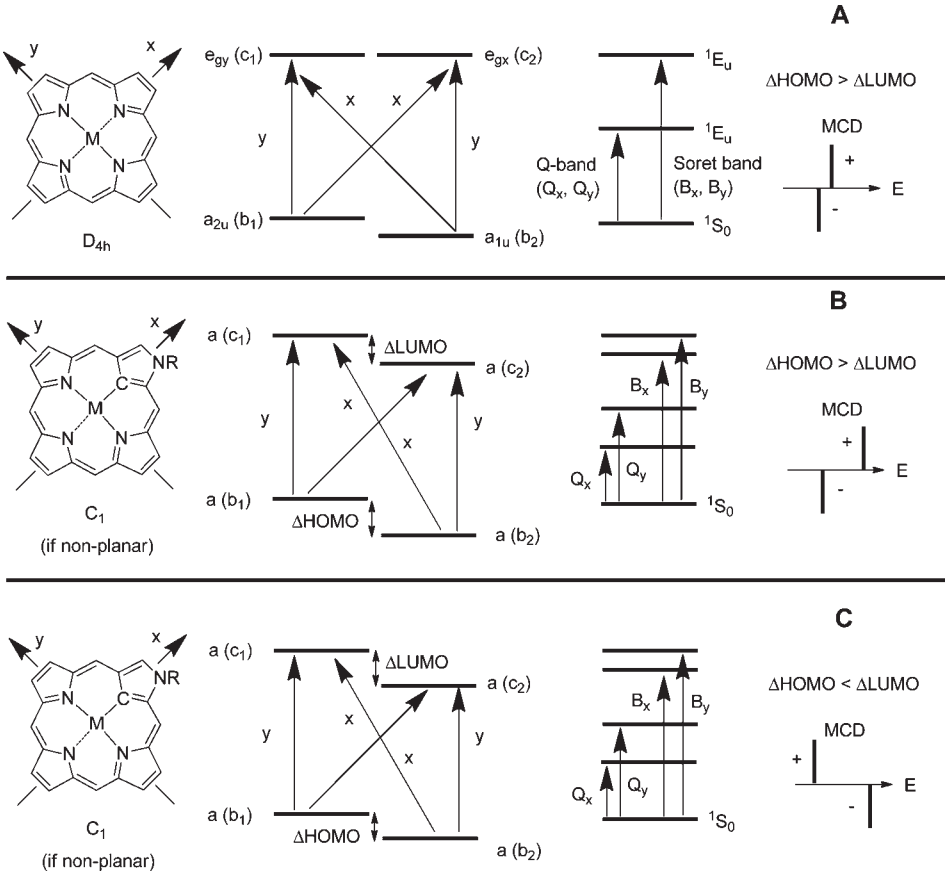

Figure 1. Simplified Gouterman's four-orbital model and Michl's perimeter model for D_{4h} symmetric porphyrins (A) and two possible cases expected for C_1 symmetric *N*-confused porphyrins (B and C).

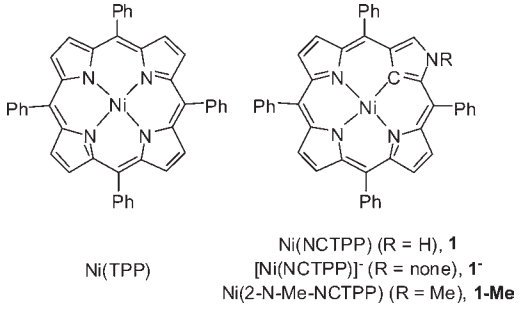

Figure 2. Nickel *N*-confused porphyrins (right) and parent nickel tetraphenylporphyrin (left).

manipulated to invert the ΔLUMO to ΔHOMO relationship. In this report, we present the first MCD study on nickel *N*-confused porphyrin **1**, its 2-*N*-methyl derivative **1-Me**, and the deprotonated form of **1** (**1**$^-$, Figure 2), which was further complimented with UV−vis spectroscopy as well as DFT, time-dependent DFT (TDDFT), and semiempirical ZINDO/S calculations. Our experimental and theoretical data shown below suggest that the simple and reversible deprotonation of the external NH proton in **1** dramatically changes the electronic structure of the porphyrin core from the ΔHOMO < ΔLUMO to the ΔHOMO > ΔLUMO relationship. Such change, in return, results in a change of the sign-reversed MCD pattern observed in **1** and **Me-1** into one usually observed for the *meso*-(tetraaryl)porphyrins MCD pattern of **1**$^-$.

EXPERIMENTAL SECTION

Synthesis and Instrumentation. All solvents were purchased from commercial sources and dried using standard approaches prior to experiments. A methanol solution of $(NBu_4)OH$ was purchased from Aldrich used without future purification. *N*-Confused porphyrin was synthesized as described by Lindsey and Geier.[10] Methylation of the inverted pyrrole at the external nitrogen position was carried out as previously described,[11] and nickel ion was inserted using the method developed by Latos-Grażyński.[1b] UV−vis−NIR data were obtained on a JACSO V-670 or Cary 17 spectrometer in dichloromethane as solvent. MCD data were recorded using an OLIS DCM 17 CD spectropolarimeter using a permanent 1.4 T DeSa magnet. The spectra were recorded twice for each sample, once with a parallel field and again with an antiparallel field, and their intensities were expressed by molar ellipticity per $T = [\Theta]_M/\text{deg M}^{-1}\text{ cm}^{-1}\text{ T}^{-1}$.

Computational Aspects. All DFT calculations were conducted using the Gaussian 03 software package running under either a Windows or UNIX OS.[12] The molecular geometries were obtained via optimization with Becke's exchange functional[13] and Perdew 86 nonlocal correlation functional (BP86)[14] coupled with 6-31G(d) basis set[15] for all atoms. For all optimized structures, frequency calculations were carried out to ensure that optimized geometries represented local minima. In agreement with available X-ray crystal data for *N*-confused porphyrins, phenyl rings in optimized **1** and **Me-1** compounds are not perfectly perpendicular to the porphyrin core. All our attempts to force these substituents into perpendicular positions result in higher energy structures. When necessary, the percent contributions of atomic orbitals to molecular orbitals were calculated using the VMOdes program.[16]

dx.doi.org/10.1021/ic102255k |*Inorg. Chem.* 2011, 50, 6902–6909

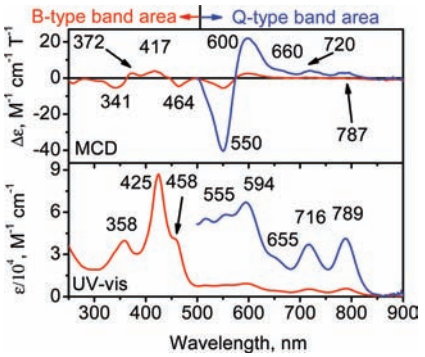

Figure 3. Experimental MCD (top) and UV−vis (bottom) spectra of complex **1**.

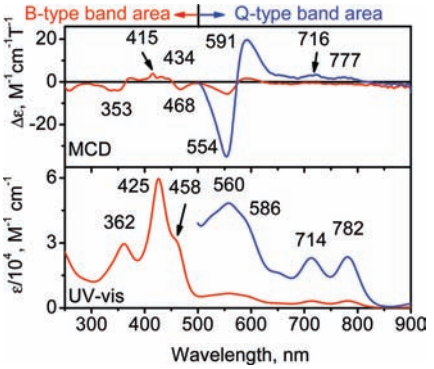

Figure 4. Experimental MCD (top) and UV−vis (bottom) spectra of complex **1-Me**.

TDDFT calculations were conducted at the same level of theory as geometry optimizations and single point calculations. The first 50 excited states were calculated in order to ensure that both Q- and B-band regions of the UV−vis spectrum are covered. ZINDO/S calculations[17] for **1**, **Me-1**, and **1**$^-$ complexes were conducted using Gaussian 03 software. Since MCD spectra cannot be calculated using commercially available ZINDO/S software, MCD calculations were conducted using the ZINDO/S program provided by Joseph Michl. Since this code cannot handle d-orbitals, the nickel atom in **1**, **Me-1**, and **1**$^-$ complexes was replaced by magnesium. Since we were interested in *N*-confused porphyrin centered $\pi-\pi^*$ transitions, such an approach is valid as long as the energies and compositions of these transitions are close to each other. Our comparative calculations on the UV−vis spectra and electronic structures of nickel and magnesium complexes of **1**, **Me-1**, and **1**$^-$ using the ZINDO/S approach indeed result in almost identical results for $\pi-\pi^*$ transitions and orbital energies (Supporting Information).

RESULTS AND DISCUSSION

Nickel *N*-confused porphyrins **1** and **1-Me** (Figure 2) can be readily generated via published methods.[1,10] The 2-*N*-methyl derivative (**1-Me**), which has the alkyl group on the external nitrogen position, can be synthesized via methylation of free base *N*-confused porphyrin[11] followed by standard nickel metalation.[1b] In both cases, the structures of the two compounds are nearly identical, but the presence of the external methyl group prevents deprotonation and formation of the trianionic tautomeric form of the macrocycle.

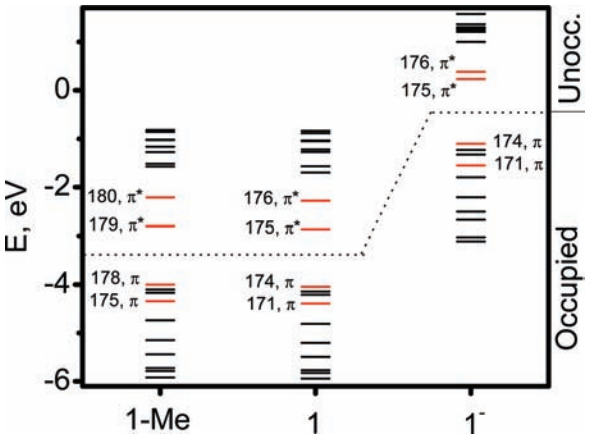

Figure 5. DFT predicted orbital energies of **1**, **1-Me**, and **1**$^-$. Gouterman's four-orbital model MOs are given in red.

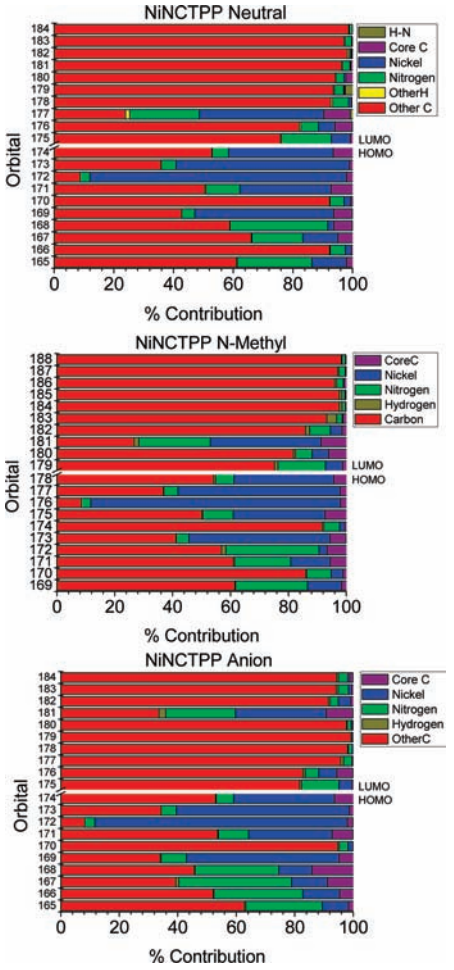

Figure 6. Molecular orbital compositions for frontier orbitals in **1**, **1-Me**, and **1**$^-$ predicted at the DFT level.

The UV−vis and MCD spectra of **1** and **1-Me** are very similar to each other and appear in Figures 3 and 4. Unlike the regular tetraaryl-containing transition-metal porphyrins, which have an intense Soret band at ~420 nm and a weak Q-band at ~600 nm, the UV−vis spectra of **1** and **1-Me** are more complex. Specifically, the Soret band has a prominent shoulder at ~460 nm,

dx.doi.org/10.1021/ic102255k |*Inorg. Chem.* 2011, 50, 6902–6909

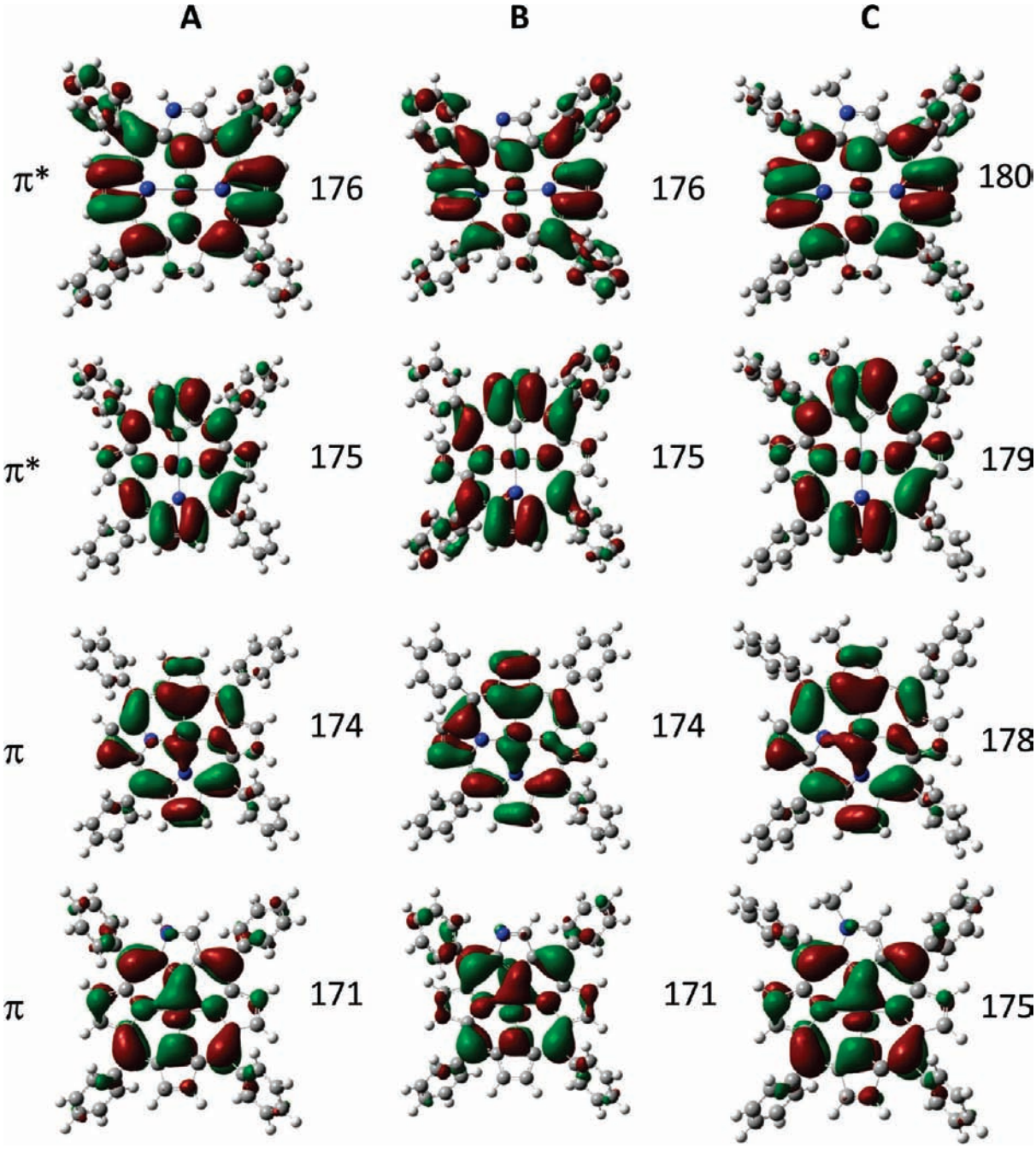

Figure 7. Gouterman's type frontier orbitals calculated for **1** (A), **1-Me** (B), and $\mathbf{1}^-$ (C) at the DFT level.

several overlapping bands are observed between 500 and 600 nm, and two prominent low-energy bands are observed at ~720 and ~790 nm. In the absence of degenerate excited states and paramagnetic centers in **1** and **1-Me**, their MCD spectra could be described using Faraday *B* terms, which originate from magnetically induced mixing of nondegenerate excited states. The intensities of the MCD signals in the Q-band region are close to those observed for the Soret band region, reflecting large angular momentum properties in the former transitions. The most striking feature of the MCD spectra of **1** and **1-Me** is the unusual positive-to-negative sign sequence for ascending energy observed in the Q-band region. Indeed, all bands and shoulders between 750 and 560 nm have positive amplitudes following bands and shoulders between 560 and 500 nm with negative amplitudes. Such MCD sign sequence is in contrast to that observed in most transition-metal porphyrins in which the lowest energy bands have negative amplitudes of MCD terms and reflects larger energy difference between the porphyrin core-centered LUMO and LUMO+1 π^* MOs (ΔLUMO) than between the porphyrin core-centered HOMO and HOMO−1 π MOs (ΔHOMO).

In order to confirm an unusual ΔLUMO > ΔHOMO relationship in **1** and **1-Me** and to gain further insight into the experimental UV−vis and MCD data, we have conducted DFT, TDDFT, and semiempirical ZINDO/S calculations, which have proven to be reliable in calculation of the vertical excitation

dx.doi.org/10.1021/ic102255k |*Inorg. Chem.* 2011, 50, 6902–6909

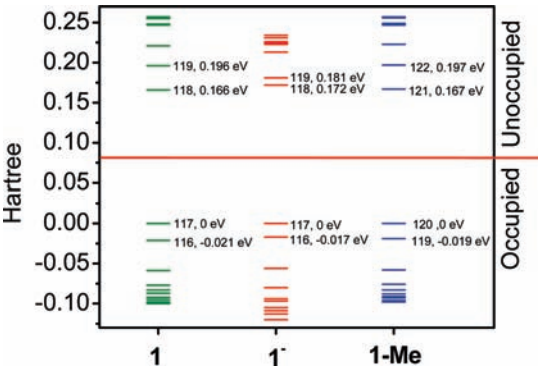

Figure 8. Orbital energies of **1**, **1-Me**, and **1**$^-$ calculated at ZINDO/S level and normalized to the energy of the HOMOs.

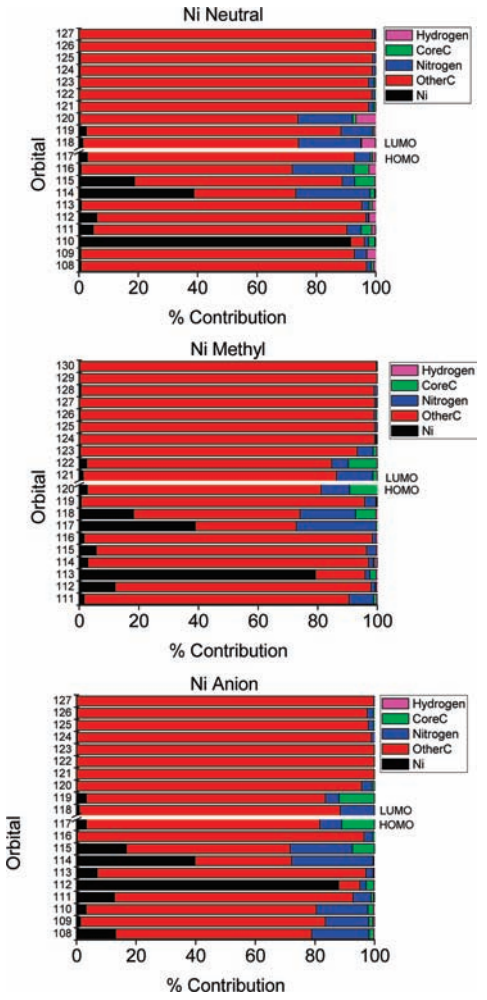

Figure 9. Molecular orbital compositions for frontier orbitals in **1**, **1-Me**, and **1**$^-$ predicted at the ZINDO/S level.

energies of porphyrinoid systems.[18] Both DFT (Figures 5−7) and ZINDO/S (Figure 8 and 9) calculations are in agreement with the experimental MCD spectra of **1** and **1-Me**. In particular, within the borders of Gouterman's four-orbital model, values calculated for **1** were ΔLUMO (0.60 eV, DFT; 0.82 eV, ZINDO/S) > ΔHOMO (0.35 eV, DFT; 0.57 eV, ZINDO/S). A similar relationship was also predicted for **1-Me**: ΔLUMO (0.60 eV, DFT; 0.82 eV, ZINDO/S) > ΔHOMO (0.34 eV, DFT; 0.52 eV, ZINDO/S). Moreover, from DFT and semiempirical calculations, it seems that the influence of the methyl group attached to the external pyrrolic nitrogen in **1-Me** is small, in agreement with UV−vis and MCD data. Further insight into the UV−vis and MCD spectroscopy of complexes **1** and **Me-1** was gained on the basis of TDDFT and ZINDO/S calculations. TDDFT calculations on **1** and **1-Me** (Figures 11 and 12) predict nine bands between 500 and 1000 nm region with all of them having some contributions from classic Gouterman's four-orbital model transitions. In both **1** and **1-Me** complexes, the lowest energy excited state predominantly consists of HOMO → LUMO (π to π^*) transition and thus was assigned to the Q_x band. The presence of the nickel-centered MOs between HOMO (π) and HOMO−3 (π) results in two low-intensity MLCT bands predicted between 700 and 900 nm. Excited state 4 again is dominated by the Gouterman's type $\pi \rightarrow \pi^*$ transitions and thus was assigned to the Q_y band. Since the semiempirical ZINDO/S method lowers the energies of the metal-centered MOs compared to the porphyrin-centered π MOs, the only $\pi \rightarrow \pi^*$ transitions predicted by this method were in the 500−900 nm region, with both being Gouterman's type $\pi \rightarrow \pi^*$ transitions (Figures 11 and 12). Again, the first excited state is dominated by the HOMO → LUMO $\pi \rightarrow \pi^*$ transition and thus was assigned to the Q_x band. The second excited state was assigned to the Q_y band. More importantly, the ZINDO/S approach predicts a positive amplitude for the low-energy Q_x band and negative amplitude for the

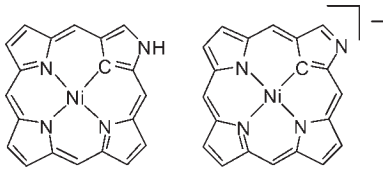

Figure 10. Proposed alteration of the tautomeric state upon deprotonation of the peripheral nitrogen.

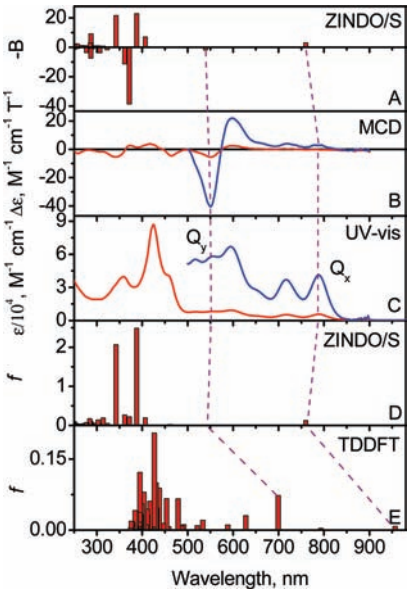

Figure 11. Predicted ZINDO/S MCD B terms (A), experimental MCD (B), experimental UV−vis (C), calculated ZINDO/S (D), and calculated TDDFT (E) vertical excitation energies for **1**.

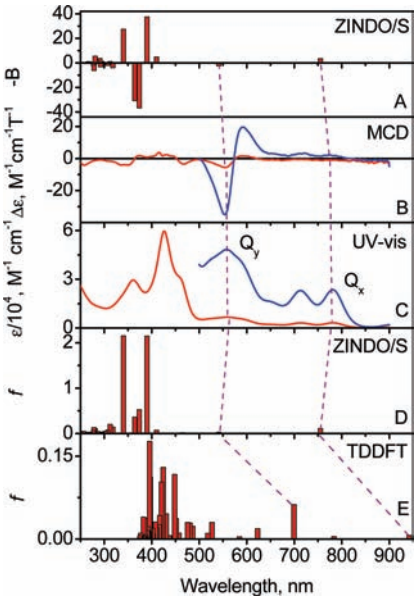

Figure 12. Predicted ZINDO/S MCD B terms (A), experimental MCD (B), experimental UV−vis (C), calculated ZINDO/S (D), and calculated TDDFT (E) vertical excitation energies for **1-Me**.

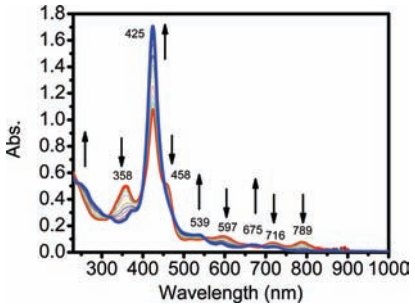

Figure 13. Transformation of **1** (red) into **1**$^-$ (blue) during titration with $(NBu_4)OH$ in a DCM−MeOH mixture.

higher energy Q_y band, in agreement with Michl's perimeter model and experimental MCD spectra of **1** and **1-Me**.

Both DFT and semiempirical ZINDO/S calculations suggest that the nitrogen atom of the inverted pyrrolic ring makes a significant contribution to the porphyrin core-centered π HOMO and π^* LUMO, but not to the porphyrin core-centered π HOMO-1 and π^* LUMO+1. Since both the HOMO and LUMO in **1** and **1-Me** have a significant contribution from the external nitrogen atom of the inverted pyrrolic ring, an increase of electron density on this atom would lead to larger *destabilization* of LUMO and HOMO relative to that in LUMO+1 and HOMO−1. In addition, we also surmised that deprotonation would alter the electronic structure of **1** to resemble that of the internally protonated form (Figure 10). Both situations would potentially *decrease* ΔLUMO and *increase* ΔHOMO, which could reverse the amplitudes of the MCD signals in the Q-band region to those usually observed in the transition-metal porphyrins. In order to test this hypothesis, **1** was reversibly deprotonated using $(NBu_4)OH$ as a base (Figure 13). The resulting UV−vis and MCD spectra of **1**$^-$ have three key differences compared to the UV−vis and MCD spectra of **1** and **1-Me**

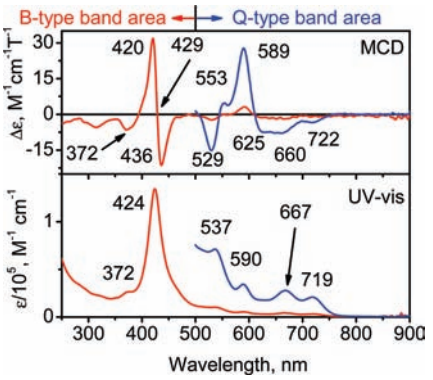

Figure 14. Experimental MCD (top) and UV−vis (bottom) spectra of complex **1**$^-$.

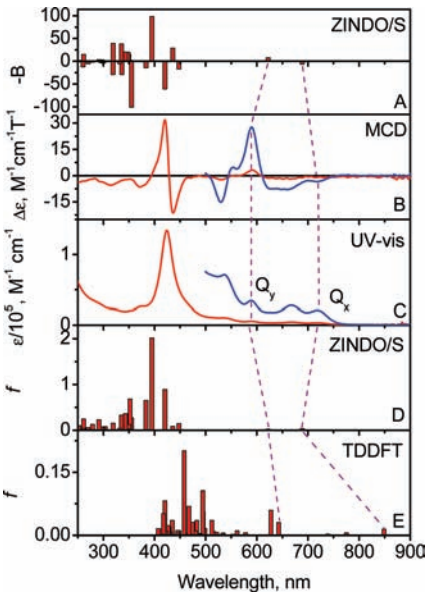

Figure 15. Predicted ZINDO/S MCD B terms (A), experimental MCD (B), experimental UV−vis (C), calculated ZINDO/S (D), and calculated TDDFT (E) vertical excitation energies for **1**$^-$.

(Figures 13 and 14). First, the UV−vis spectrum of **1**$^-$ is closer to the usual spectrum of tetraarylporphyrins. Indeed, upon deprotonation of **1**, the Soret band shoulder at 458 nm and the intense band at 358 nm disappear, followed by an increase of the Soret band intensity. In addition, an unusual for the tetraarylporphyrins low-energy band at 789 nm disappears, and the lowest energy band in **1**$^-$ appears as usual for tetraarylporphyrins in the region of 719 nm. Second, similar to other tetrarylporphyrins, the MCD spectrum of **1**$^-$ is dominated by the Soret band region, which is about one order of magnitude more intense compared to the Q-band region signals. Finally, negative-to-positive in ascending energy Faraday *B* terms were observed in the Q-band region of **1**$^-$, suggesting the usual for porphyrins ΔLUMO < ΔHOMO relationship in **1**$^-$. Such a simple possibility for manipulation of the electronic structure in **1** was further confirmed by DFT and ZINDO/S calculations (Figures 5−9 and 15). Indeed, within the borders of Gouterman's four-orbital model, values calculated for **1**$^-$ were ΔLUMO (0.20 eV, DFT; 0.24 eV, ZINDO/S) < ΔHOMO (0.45 eV, DFT; 0.46 eV, ZINDO/S). In agreement with our hypothesis, all four Gouterman's type MOs are

dx.doi.org/10.1021/ic102255k |*Inorg. Chem.* 2011, 50, 6902–6909

significantly destabilized in $\mathbf{1}^-$ compared to **1**, but a larger destabilization of LUMO and HOMO is, indeed, responsible for a new ΔLUMO < ΔHOMO relationship. TDDFT and ZINDO/S calculations on $\mathbf{1}^-$ are in agreement with its electronic structure. Thus, TDDFT calculations on $\mathbf{1}^-$ predict 10 bands between the 500 and 1000 nm region, with all of them having contributions from classic Gouterman's four-orbital model transitions. The first excited state is dominated by the HOMO → LUMO ($\pi \rightarrow \pi^*$) transition and thus was assigned to the Q_x band (Figure 15). Similar to complexes **1** and **Me-1**, low-intensity transitions 2 and 3 have predominant MLCT character, while excited state 4 fits well within Gouterman's four-orbital model and thus was assigned as the Q_y band. Again, as predicted by ZINDO/S method, energies of the metal-centered MOs are significantly lower compared to the π MOs and thus both predicted in the 500−900 nm region excited states were assigned as Q-bands. The first one is dominated by the HOMO → LUMO ($\pi \rightarrow \pi^*$) transition and thus was assigned as a Q_x band, while the second excited state was assigned as a Q_y band (Figure 15). More importantly,the ZINDO/S approach predicts a negative amplitude for the low-energy Q_x band and positive amplitude for the higher energy Q_y band, in agreement with Michl's perimeter model and experimental MCD spectra of $\mathbf{1}^-$.

CONCLUSIONS

In conclusion, nickel *N*-confused porphyrins **1** and **1-Me** exhibit a rare MCD spectra compared to those observed in other metalloporphyrins and modified variants. The frontier orbital structures of compounds **1** and **1-Me** deviate from that predicted by the Gouterman's four-orbital model, which predicts a significant separation between the HOMO and HOMO−1 and a degenerate (or nearly degenerate) LUMO and LUMO+1. The inversion of two atom positions in *N*-confused porphyrin relative to normal porphyrin greatly affects the electronic structure of the macrocycle by altering one of the two conjugation pathways and by inducing asymmetry in the macrocycle. As a result, the LUMO and LUMO+1 orbitals lose their degeneracy and exhibit a larger gap than observed in the HOMO/HOMO−1 pair. We also showed that a simple deprotonation of the external pyrrolic protons could easily change the electronic structure of **1** from ΔLUMO > ΔHOMO to the usual ΔLUMO < ΔHOMO, which could only be confirmed experimentally by MCD spectroscopy.

ASSOCIATED CONTENT

Supporting Information. Optimized coordinates for target compounds. Figures 11, 12, and 15 plotted on an energy scale. This material is available free of charge via the Internet at http://pubs.acs.org.

AUTHOR INFORMATION

Corresponding Author

*E-mail: ziegler@uakron.edu (C.J.Z.), vnemykin@d.umn.edu (V.N.N).

ACKNOWLEDGMENT

C.J.Z. acknowledges the National Science Foundation for support of this research. (CHE-0616416). Minnesota Supercomputing Institute and the National Science Foundation (CHE-0809203) support for V.N.N. are greatly appreciated. V.N.N. is also thankful to Prof. J. Michl for his original ZINDO/S MCD codes.

REFERENCES

(1) (a) Furuta, H.; Asano, T.; Ogawa, T. *J. Am. Chem. Soc.* **1994**, *116*, 767. (b) Chmielewski, P. J.; Latos-Grażyński, L.; Rachlewicz, K.; Glowiak, T. *Angew. Chem., Int. Ed.* **1994**, *33*, 779–781.

(2) (a) Furuta, H.; Maeda, H.; Osuka, A. *Chem. Commun.* **2002**, 1795–1804. (b) Chmielewski, P. J.; Latos-Grażyński, L. *Coord. Chem. Rev.* **2005**, *249*, 2510–2533.(c) Latos-Grażyński, L. Core Modified Heteroanalogues of Porphyrins and Metalloporphyrins. In *The Porphyrin Handbook*; Kadish, K. M., Smith, K. M., Guilard, R., Eds.; Academic Press: New York, 2000; pp 361−416. (d) Harvey, J. D.; Ziegler, C. J. *Coord. Chem. Rev.* **2003**, *247*, 1–19. (e) Pawlicki, M.; Latos-Grażyński, L. *Chem. Rec.* **2006**, *6*, 64–78. (f) Srinivasan, A.; Furuta, H. *Acc. Chem. Res.* **2005**, *38*, 10–20. (g) Maeda, H.; Furuta, H. *Pure Appl. Chem.* **2006**, *78*, 29–44. (h) Harvey, J. D.; Ziegler, C. J. *J. Inorg. Biochem.* **2006**, *100*, 869–880.

(3) (a) Alemán, E. A.; Rajesh, C. S.; Ziegler, C. S.; Modarelli, D. A. *J. Phys. Chem.* **2006**, *110*, 8605–8612. (b) Belair, J. P.; Ziegler, C. S.; Rajesh, C. S.; Modarelli, D. A. *J. Phys. Chem. A* **2002**, *106*, 6445–6451. (c) Vyas, S.; Hadad, C. M.; Modarelli, D. A. *J. Phys. Chem. A* **2008**, *112* (29), 6533–6549. (d) Shaw, J. L.; Garrison, S. A.; Aleman, E. A.; Ziegler, C. J.; Modarelli, D. A. *J. Org. Chem.* **2004**, *69*, 7423. (e) Parusel, A. B. J.; Ghosh, A. J. *Phys. Chem. A* **2000**, *104*, 2504–2507. (f) Ghosh, A.; Wondimagegn, T.; Nilsen, H. *J. Phys. Chem. B* **1998**, *102*, 10459–10467. (g) Zandler, M. E.; D'Souza, F. *J. Mol. Struct. (THEOCHEM)* **1997**, *401*, 301–314. (h) Szterenberg, L.; Latos-Grażyński, L. *Inorg. Chem.* **1997**, *36*, 6287–6291.

(4) (a) Kobayashi, N.; Nakai, K. *Chem. Commun.* **2007**, 4077. (b) Mack, J.; Stillman, M. J.; Kobayashi, N. *Coord. Chem. Rev.* **2007**, *251*, 429. (c) Nemykin, V. N.; Rohde, G. T.; Barrett, C. D.; Hadt, R. G.; Sabin, J. R.; Reina, G.; Galloni, P.; Floris, B. *Inorg. Chem.* **2010**, *49*, 7497–7509. (d) Nemykin, V. N.; Rohde, G. T.; Barrett, C. D.; Hadt, R. G.; Bizzarri, C.; Galloni, P.; Floris, B.; Nowik, I.; Herber, R. H.; Marrani, A. G.; Zanoni, R.; Loim, N. M. *J. Am. Chem. Soc.* **2009**, *131*, 14969–14978. (e) Nemykin, V. N.; Galloni, P.; Floris, B.; Barrett, C. D.; Hadt, R. G.; Subbotin, R. I.; Marrani, A. G.; Zanoni, R.; Loim, N. M. *Dalton Trans.* **2008**, 4233–4246. (f) Nemykin, V. N.; Kobayashi, N. *Chem. Commun.* **2001**, 165–166. (g) Gorski, A.; Vogel, E.; Sessler, J. L.; Waluk, J. *J. Phys. Chem. A* **2002**, *106*, 8139. (h) Lukyanets, E. A.; Nemykin, V. N. *J. Porphyrins Phthalocyanines* **2010**, *14*, 1–40. (i) Mack, J.; Bunya, M.; Lansky, D.; Goldberg, D. P.; Kobayashi, N. *Heterocycles* **2008**, *76*, 1369–1380. (j) Stillman, M.; Mack, J.; Kobayashi, N. *J. Porphyrins Phthalocyanines* **2002**, *6*, 296–300. (k) Nakamura, Y.; Aratani, N.; Shinokubo, H.; Takagi, A.; Kawai, T.; Matsumoto, T.; Yoon, Z. S.; Kim, D. Y.; Ahn, T. K.; Kim, D.; Kobayashi, N. *J. Am. Chem. Soc.* **2006**, *128*, 4119–4127. (l) Kuzuhara, D.; Mack, J.; Yamada, H.; Okujima, T.; Ono, N.; Kobayashi, N. *Chem.—Eur. J.* **2009**, *15*, 10060–10069. (m) Xue, Z.-L.; Shen, Z.; Mack, J.; Kuzuhara, D.; Yamada, H.; Okujima, T.; Ono, N.; You, X.-Z.; Kobayashi, N. *J. Am. Chem. Soc.* **2008**, *130*, 16478–16479.

(5) (a) Gouterman, M. J. In *The Porphyrins*; Dolphin, D., Ed.; Academic Press: New York, 1978; Vol. III, pp 1−165. (b) Seybold, P. G.; Gouterman, M. J. *Mol. Spectrosc.* **1969**, *31*, 1–13. (c) Gouterman, M. J. *Mol. Spectrosc.* **1961**, *6*, 138–163.

(6) (a) Waluk, J.; Michl, J. *J. Org. Chem.* **1991**, *56*, 2729. (b) Michl, J. *J. Am. Chem. Soc.* **1978**, *100*, 6801. (c) Michl, J. *J. Am. Chem. Soc.* **1978**, *100*, 6812. (d) Michl, J. *J. Am. Chem. Soc.* **1978**, *100*, 6819.

(7) (a) Mason, W. R. *A Practical Guide to Magnetic Circular Dichroism Spectroscopy*; John Wiley & Sons Inc.: New York, 2007. (b) Mack, J.; Stillman, M. J. *Coord. Chem. Rev.* **2001**, *219*−*221*, 993–1032.(c) Mack, J.; Stillman, M. J. in: *Porphyrin Handbook*; Kadish, K. M., Smith, K. M., Guilard, R., Eds.; Academic Press: New York, 2003; Vol. 16, pp 43−116.

(8) (a) Mack, J.; Asano, Y.; Kobayashi, N.; Stillman, M. J. *J. Am. Chem. Soc.* **2005**, *127*, 17697–17711. (b) Mack, J.; Bunya, M.; Shimizu, Y.;

Uoyama, H.; Komobuchi, N.; Okujima, T.; Uno, H.; Ito, S.; Stillman, M. J.; Ono, N.; Kobayashi, N. *Chem.—Eur. J.* **2008**, *14*, 5001–5020. (c) Gorski, A.; Kohler, T.; Seidel, D.; Lee, J. T.; Orzanowska, G.; Sessler, J. L.; Waluk, J. *Chem.—Eur. J.* **2005**, *11*, 4179. (d) Gorski, A.; Vogel, E.; Sessler, J. L.; Waluk, J. *Chem. Phys.* **2002**, *282*, 37. (e) Muranaka, A.; Matsushita, O.; Yoshida, K.; Mori, S.; Suzuki, M.; Furuyama, T.; Uchiyama, M.; Osuka, A.; Kobayashi, N. *Chem.—Eur. J.* **2009**, *15*, 3744. (f) Keegan, J. D.; Stolzenberg, A. M.; Lu, Y. C.; Linder, R. E.; Barth, G.; Moscowitz, A.; Bunnenberg, E.; Djerassi, C. *J. Am. Chem. Soc.* **1982**, *104*, 4305.

(9) Muranaka, A.; Homma, S.; Maeda, H.; Furuta, H.; Kobayashi, N. *Chem. Phys. Lett.* **2008**, *460*, 495–498.

(10) Geier, G. R., III.; Haynes, D. M.; Lindsey, J. S. *Org. Lett.* **1999**, *1*, 1455–1458.

(11) Qu, W.; Ding, T.; Cetin, A.; Harvey, J. D.; Taschner, M. J.; Ziegler, C. J. *J. Org. Chem.* **2006**, *71*, 811–814.

(12) Frisch, M. J.; Trucks, G. W.; Schlegel, H. B.; Scuseria, G. E.; Robb, M. A.; Cheeseman, J. R.; Montgomery, J. A., Jr.; Vreven, T.; Kudin, K. N.; Burant, J. C.; Millam, J. M.; Iyengar, S. S.; Tomasi, J.; Barone, V.; Mennucci, B.; Cossi, M.; Scalmani, G.; Rega, N.; Petersson, G. A.; Nakatsuji, H.; Hada, M.; Ehara, M.; Toyota, K.; Fukuda, R.; Hasegawa, J.; Ishida, M.; Nakajima, T.; Honda, Y.; Kitao, O.; Nakai, H.; Klene, M.; Li, X.; Knox, J. E.; Hratchian, H. P.; Cross, J. B.; Bakken, V.; Adamo, C.; Jaramillo, J.; Gomperts, R.; Stratmann, R. E.; Yazyev, O.; Austin, A. J.; Cammi, R.; Pomelli, C.; Ochterski, J.; Ayala, P. Y.; Morokuma, K.; Voth, G. A.; Salvador, P.; Dannenberg, J. J.; Zakrzewski, V. G.; Dapprich, S.; Daniels, A. D.; Strain, M. C.; Farkas, O.; Malick, D. K.; Rabuck, A. D.; Raghavachari, K.; Foresman, J. B.; Ortiz, J. V.; Cui, Q.; Baboul, A. G.; Clifford, S.; Cioslowski, J.; Stefanov, B. B.; Liu, G.; Liashenko, A.; Piskorz, P.; Komaromi, I.; R. L.Martin, Fox, D. J.; Keith, T.; Al-Laham, M. A., Peng, C. Y.; Nanayakkara, A.; Challacombe, M.; Gill, P. M. W.; Johnson, B. G.; Chen, W.; Wong, M. W.; Gonzalez, C.; Pople, J. A. *GAUSSIAN 03 (Revision C.02)*; Gaussian, Inc., Wallingford, CT, 2004.

(13) Becke, A. D. *Phys. Rev. A* **1988**, *38*, 3098.

(14) Perdew, J. P. *Phys. Rev. B* **1986**, *33*, 8822.

(15) McLean, A. D.; Chandler, G. S. *J. Chem. Phys.* **1980**, *72*, 5639.

(16) Nemykin, V. N.; Basu, P. *VMOdes: Virtual Molecular Orbital Description Program for Gaussian, GAMESS, and HyperChem*, Revision A 7.2; Univeristy of Minnesota, Duluth, MN, 2003.

(17) Zerner, M. C.; Lowe, G. H.; Kirchner, R. F.; Mueller-Westerhoff, U. T. *J. Am. Chem. Soc.* **1980**, *102*, 589.

(18) (a) Nemykin, V. N.; Hadt, R. G.; Belosludov, R. V.; Mizuseki, H.; Kawazoe, Y. *J. Phys. Chem. A* **2007**, *111*, 12901–12913. (b) Peralta, G. A.; Seth, M.; Ziegler, T. *Inorg. Chem.* **2007**, *46*, 9111–9125. (c) De Luca, G.; Romeo, A.; Scolaro, L. M.; Ricciardi, G.; Rosa, A. *Inorg. Chem.* **2009**, *48*, 8493–8507. (d) Solntsev, P. V.; Sabin, J. R.; Dammer, S. J.; Gerasimchuk, N. N.; Nemykin, V. N. *Chem. Commun.* **2010**, *46*, 6581–6583. (e) Nemykin, V. N.; Barrett, C. D.; Hadt, R. G.; Subbotin, R. I.; Maximov, A. Y.; Polshin, E. V.; Koposov, A. Y. *Dalton Trans.* **2007**, 3378–3389. (f) Nemykin, V. N.; Hadt, R. G. *J. Phys. Chem. A* **2010**, *114*, 12062–12066. (g) Improta, R.; Ferrante, C.; Bozio, R.; Barone, V. *Phys. Chem. Chem. Phys.* **2009**, *11*, 4664–4673. (h) Suvitha, A.; Belosludov, R. V.; Mizuseki, H.; Kawazoe, Y.; Takeda, M.; Kohno, M.; Ohuchi, N. *Mater. Trans.* **2008**, *49*, 2416–2419. (i) Balanay, M. P.; Kim, D. H. *Phys. Chem. Chem. Phys.* **2008**, *10*, 5121–5127. (j) Nakai, K.; Kurotobi, K.; Osuka, A.; Uchiyama, M.; Kobayashi, N. *J. Inorg. Biochem.* **2008**, *102*, 466–471. (k) Infante, I.; Lelj, F. *J. Chem. Theory Comput.* **2007**, *3*, 838–851. (l) Delaere, D.; Minh, T. N. *Chem. Phys. Lett.* **2003**, *376*, 329–337.